Acta Crystallographica Section F
Structural Biology and Crystallization Communications
ISSN 1744-3091

Expression, purification, crystallization and preliminary X-ray studies of *Lactobacillus jensenii* enolase

Paul T. Harris,‡ Kannan Raghunathan,‡ Rachel R. Spurbeck, Cindy G. Arvidson and Dennis N. Arvidson*

Michigan State University, Department of Microbiology and Molecular Genetics and Michigan State University, Center for Microbial Pathogenesis, East Lansing, MI 48824, USA

‡ These authors contributed equally.

Correspondence e-mail: arvidso4@msu.edu

Received 17 May 2010
Accepted 13 June 2010

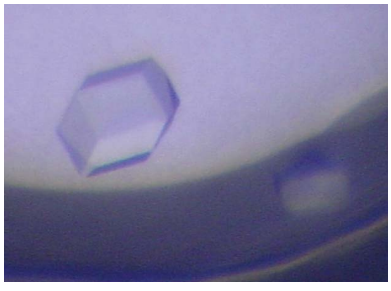

Recombinant *Lactobacillus jensenii* enolase fused to a C-terminal noncleavable His tag was expressed in *Escherichia coli*, purified and crystallized by sitting-drop vapor diffusion. A complete data set was collected to 3.25 Å resolution. The crystals belonged to space group *I*4, with unit-cell parameters $a = b = 145.31$, $c = 99.79$ Å. There were two protein subunits in the asymmetric unit, which gave a Matthews coefficient V_M of 2.8 Å^3 Da^{-1}, corresponding to 55.2% solvent content.

1. Introduction

Enolase is a cytosolic housekeeping enzyme that is involved in glycolysis. However, enolases from several organisms have additional moonlighting functions (Pancholi, 2001; Pancholi & Chhatwal, 2003; Copley, 2003). Surface-associated enolases in *Lactobacillus* species bind extracellular matrix components such as fibronectin, collagen and laminin (Castaldo *et al.*, 2009; Antikainen *et al.*, 2007*a*,*b*; Kapczynski *et al.*, 2000). Recently, a surface-associated enolase was discovered in *Lactobacillus jensenii*, which is one of the most prevalent bacterial species of the healthy human vaginal microbiota (Spurbeck & Arvidson, 2010; Zhou *et al.*, 2004). When recombinantly expressed as a His_6-tagged protein, the surface-associated enolase inhibited the adherence of *Neisseria gonorrhoeae* to epithelial cells (Spurbeck & Arvidson, 2010). Here, we describe the cloning, expression, purification, crystallization and preliminary X-ray diffraction analysis of the full-length enolase of *L. jensenii* fused to a C-terminal His_6 tag.

2. Materials and methods

2.1. Expression and purification of recombinant enolase

The enolase gene from *L. jensenii* was subcloned into the plasmid pET24a (Novagen, San Diego, USA) for expression as a C-terminal His_6-tagged protein as described previously (Spurbeck & Arvidson, 2010). Briefly, the *eno* gene was amplified by polymerase chain reaction (PCR) using the primers EnoFwd (5′-AGATTT**CATATG**-TCTGTAATTACTGATATCC-3′), which contains an *Nde*I restriction site (bold), and EnoRev (5′-AAGT**GCGGCCGC**AAATTGTT-TATGTAAATTGTAAAAAC-3′), which contains a *Not*I restriction site (bold). Both the PCR product and the plasmid pET24a were digested with *Nde*I and *Not*I restriction enzymes (New England Biolabs, Ipswich, Massachusetts, USA). The ligation mixture was transformed into chemically competent *Escherichia coli* DH5α and insertion was confirmed by PCR using T7 promoter and T7 terminator primers. Using the Qiagen Miniprep kit, the plasmid containing the insert was isolated. The identity of the insert was confirmed by sequencing. The final construct (pET24a-eno) encodes the full-length enolase protein with a C-terminal His tag LEHHHHHH. pET24a-eno was transformed into chemically competent *E. coli* BL21λDE3 for expression. Cultures of *E. coli* BL21λDE3 carrying pET24a-eno were grown overnight in 20 ml LB medium supplemented with 50 mg l^{-1} kanamycin and were used to inoculate 1.5 l ZY-5052 auto-inducing medium (Studier, 2005) also supplemented with 50 mg l^{-1} kanamycin. After overnight growth at 301 K with shaking at 200 rev min^{-1}, the cells were pelleted by centrifugation. The cells

were then resuspended in 50 m*M* NaH_2PO_4 pH 7.0, 300 m*M* NaCl and lysed by shearing at 138 MPa with an M-110P Processor (Microfluidics Corp., Newton, Masssachusetts, USA).

Insoluble material was removed by centrifugation and the crude lysate was loaded onto an Ni–NTA resin column (BD Biosciences, San Jose, California, USA) previously equilibrated with 50 m*M* NaH_2PO_4 pH 7.0, 300 m*M* NaCl. The column was washed with 50 m*M* NaH_2PO_4 pH 7.0, 300 m*M* NaCl, 10 m*M* imidazole and bound protein was eluted with 50 m*M* NaH_2PO_4 pH 7.0, 300 m*M* NaCl, 250 m*M* imidazole. The protein was then dialyzed against 50 m*M* NaH_2PO_4 pH 7.0, 25 m*M* NaCl using 3350 Da molecular-weight cutoff dialysis tubing (Spectrum Laboratories Inc., Rancho Dominguez, California, USA) and loaded onto an anion-exchange column (Bio-Rad, Hercules, California, USA) equilibrated with 50 m*M* NaH_2PO_4 pH 7.0, 10 m*M* NaCl. Upon elution using 50 m*M* NaH_2PO_4 pH 7.0 with a 100–900 m*M* NaCl gradient, the protein was dialyzed into 15 m*M* Tris pH 7.5, 200 m*M* NaCl. The protein was concentrated in a 50 ml stirred-cell Amicon ultrafiltration unit under 448 kPa O_2-free N_2 using a YM-30 30 kDa molecular-weight cutoff membrane (Millipore, Billerica, Massachusetts, USA). Crystallization trials were conducted using protein at a concentration of 2–4 mg ml^{-1}.

2.2. Crystallization screening and optimization

Screening was performed by sitting-drop vapor diffusion using an ORYX-4 crystallization robot (Douglas Instruments, UK) in 96-well CrystalEX vapor-diffusion plates (Corning, Lowell, Massachusetts, USA) using reservoirs filled with 70 µl of each screening condition. Trial conditions were prepared corresponding to Crystal Screens I and II (Hampton Research, Aliso Viejo, California, USA) and Wizard Screens I and II (Emerald BioSystems, Bainbridge Island, Washington, USA). For each sitting drop, 1 µl protein solution was mixed with an equal amount of screening condition drawn from the larger reservoir. The plate was then sealed with clear tape (Henkel Consumer Adhesives, Avon, Ohio, USA) and incubated at 295 K.

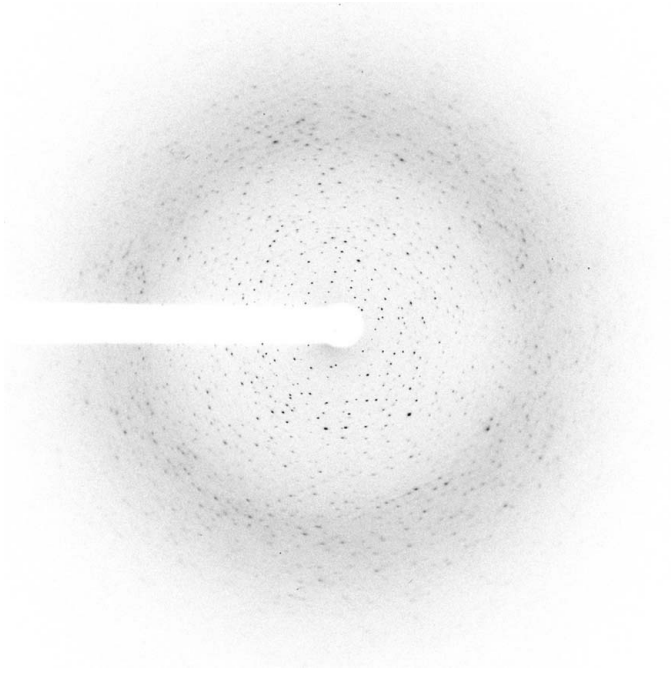

Figure 1
Diffraction pattern obtained using synchrotron radiation on the LS-CAT 2I-ID-F beamline at the Advanced Photon Source, Argonne National Laboratory, Illinois, USA.

2.3. X-ray diffraction data collection and processing

Crystals were mounted in nylon loops (Hampton Research), dragged briefly through paraffin oil and flash-cooled by dipping them in liquid nitrogen, in which they were subsequently stored. Data were collected at 100 K using a MAR CCD detector on the LS-CAT 21-ID-F beamline at the Advanced Photon Source (Fig. 1) and were processed using *HKL*-2000 (Otwinowski & Minor, 1997).

3. Results and discussion

Full-length enolase protein appended with a C-terminal His_6 tag was expressed from the plasmid pET24a-eno and purified using metal-affinity and ion-exchange chromatography (Fig. 2). Additional bands were observed in some preparations, but this did not influence crystal growth.

While Crystal Screens I and II (Hampton Research) as well as Wizard Screens I and II (Emerald BioSystems) produced many trial solutions containing microcrystals, the largest crystals formed overnight when 1 µl protein solution was equilibrated against an empty reservoir. The crystals were verified to be composed of protein using IZIT dye (Hampton Research) and the melt test (Raghunathan *et al.*, 2010) and crystal growth was reproduced using silanized glass cover slips suspended over the empty wells of VDX plates (Hampton Research). Cryoprotection was achieved by using a nylon loop to drag the crystal through a solution of paraffin oil. The resulting diffraction-quality crystals (Fig. 3) belonged to space group *I*4, with unit-cell parameters $a = b = 145.31$, $c = 99.79$ Å (Table 1). There were two protein subunits in the asymmetric unit, which gave a Matthews

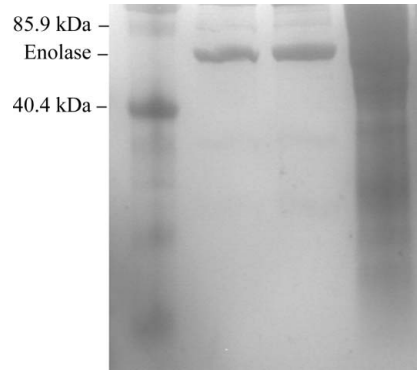

Figure 2
A tricine SDS–PAGE gel of the enolase purification, showing (from left to right) the Kaleidoscope ladder (Bio-Rad), the pooled peak fractions, the peak fraction and the crude lysate.

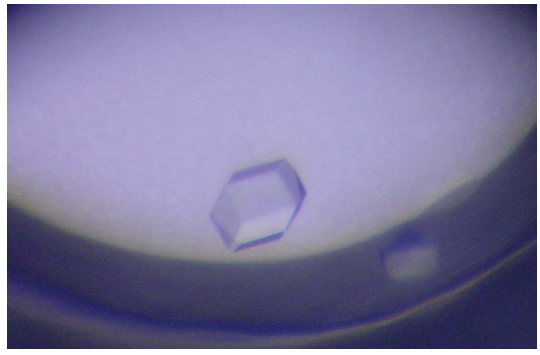

Figure 3
A crystal of enolase of approximately 0.2 mm per side.

Table 1
Data-collection statistics.

Values in parentheses are for the highest resolution shell (3.31–3.25 Å).

Wavelength (Å)	0.978
Resolution (Å)	30–3.25 (3.31–3.25)
No. of reflections	61438 (3162)
No. of unique reflections	16609 (832)
Redundancy	3.7 (3.8)
$R_{\rm merge}$ (%)†	13.1 (54.2)
Completeness (%)	99.4 (99.8)
Mean $I/\sigma(I)$	10.29 (2.06)
Mosaicity (°)	0.30

† $R_{\rm merge} = \sum_{hkl}\sum_i |I_i(hkl) - \langle I(hkl)\rangle| / \sum_{hkl}\sum_i I_i(hkl)$, where $I_i(hkl)$ is the intensity of the ith replicate of reflection hkl and $\langle I(hkl)\rangle$ is the mean value and the summations are over all i replicates and then over all hkl.

coefficient $V_{\rm M}$ of 2.8 Å^3 Da^{-1}, corresponding to 55.2% solvent content (Matthews, 1968).

The structure of enolase from *Enterococcus hirae* has previously been reported (Hosaka *et al.*, 2003). These crystals also belonged to space group $I4$, with similar unit-cell parameters $a = b = 153.51$, $c = 90.66$ Å, and diffracted to 2.80 Å resolution. Using chain A of this structure (PDB code 1iyx), the molecular-replacement program *Phaser* (McCoy *et al.*, 2007) found an initial solution with an rotation-function Z score of 13.7 and a translation-function Z score of 15.8.

The authors wish to thank Michael Garavito for assistance with the crystallization robot and Joseph Brunzelle for data-collection assistance at LS-CAT. This work was supported by Michigan State University's Center for Microbial Pathogenesis and the Research Training Program for Undergraduate Students in Biological and Mathematical Sciences program sponsored by the National Science Foundation (DMS-0531898) and Michigan State University. Use of the LS-CAT 21-ID-F beamline at the Advanced Photon Source was supported by the United States Department of Energy, Office of Science, Office of Basic Energy Sciences under Contract No. W-31-109-Eng-38. LS-CAT is supported in part by the Michigan Economic Development Corporation and the Michigan Technology Tri-Corridor Grant 085P1000817.

References

Antikainen, J., Kuparinen, V., Lahteenmaki, K. & Korhonen, T. K. (2007*a*). *FEMS Immunol. Med. Microbiol.* **51**, 526–534.
Antikainen, J., Kuparinen, V., Lahteenmaki, K. & Korhonen, T. K. (2007*b*). *J. Bacteriol.* **189**, 4539–4543.
Castaldo, C., Vastano, V., Siciliano, R. A., Candela, M., Vici, M., Muscariello, L., Marasco, R. & Sacco, M. (2009). *Microb. Cell Fact.* **8**, 14.
Copley, S. D. (2003). *Curr. Opin. Chem. Biol.* **7**, 265–272.
Hosaka, T., Meguro, T., Yamato, I. & Shirakihara, Y. (2003). *J. Biochem.* **133**, 817–823.
Kapczynski, D. R., Meinersmann, R. J. & Lee, M. D. (2000). *Curr. Microbiol.* **41**, 136–141.
Matthews, B. W. (1968). *J. Mol. Biol.* **33**, 491–497.
McCoy, A. J., Grosse-Kunstleve, R. W., Adams, P. D., Winn, M. D., Storoni, L. C. & Read, R. J. (2007). *J. Appl. Cryst.* **40**, 658–674.
Otwinowski, Z. & Minor, W. (1997). *Methods Enzymol.* **276**, 307–326.
Pancholi, V. (2001). *Cell. Mol. Life Sci.* **58**, 902–920.
Pancholi, V. & Chhatwal, G. S. (2003). *Int. J. Med. Microbiol.* **293**, 391–401.
Raghunathan, K., Harris, P. T. & Arvidson, D. N. (2010). *Acta Cryst.* F**66**, 615–620.
Spurbeck, R. R. & Arvidson, C. G. (2010). *Infect. Immun.* **78**, 3103–3111.
Studier, F. W. (2005). *Protein Expr. Purif.* **41**, 207–234.
Zhou, X., Bent, S. J., Schneider, M. G., Davis, C. C., Islam, M. R. & Forney, L. J. (2004). *Microbiology*, **150**, 2565–2573.